Diffusive Isotopic Contamination of Mafic Magma by Coexisting Silicic Liquid in the Muskox Intrusion

BRIAN W. STEWART* AND DONALD J. DEPAOLO

Shifts in ^{87}Sr/^{86}Sr and ^{143}Nd/^{144}Nd ratios measured in cumulates from the upper levels of the Muskox mafic intrusion indicate that isotopic and bulk chemical exchange were decoupled across a mafic-silicic liquid interface during crystallization of the intrusion. Modeling of diffusive exchange between liquid layers demonstrates that isotopic compositions of silicate liquids in layered magma chambers may be strongly affected by this process on time scales of 10^3 to 10^4 years. Diffusive contamination can be used to place constraints on the physical processes and time scales of magmatic systems.

CHEMICAL DIFFUSION IS GENERALLY thought not to be important in magma evolution, because the effective diffusivities of most elements are small in comparison to the length scales of magma chambers. However, recent studies of magma chamber dynamics (*1–4*) show that low-density, silica-rich magma can be maintained for a long time as a stable layer over denser mafic magma with a sharp compositional interface between the two and little mechanical mixing. In this situation, diffusion need operate only over the short distances of the compositional boundary layer between the two magma layers. Even with a thin boundary layer, chemical diffusion is minimal and the concentrations of elements within each layer are negligibly affected by the presence of the adjacent layer (*5–7*). Isotopic ratios, however, can be more strongly affected by diffusion, because diffusion of isotopic ratios occurs independently of diffusion of concentrations (*8, 9*), and effective diffusivities of isotopic ratios are not ultimately controlled by the especially slow diffusion of the major components SiO_2 and Al_2O_3 (*10, 11*). Our isotopic data from the Muskox intrusion demonstrate that measurable diffusive isotopic exchange occurs between mafic and silicic magma layers in magma chambers.

The Muskox intrusion is a prism-form layered mafic intrusion exposed along the Arctic Circle in Northwest Territories, Canada. The ultramafic and mafic cumulates that form most of the intrusion reach a thickness of ~2000 m and may thicken northward where the intrusion dips beneath its sedimentary cover. Muskox intrusion cumulates crystallized from a series of 25 injections of magma into a shallow chamber (*12, 13*). Each successive injection pushed some or all of the previously existing magma out of the chamber and formed a new cyclic unit characterized by repetitions in the cumulate stratigraphy and shifts in crystallization parameters such as the Mg/Fe ratio and the Ni concentration in olivine. Complete crystallization of the final magma injection yielded a cyclic unit (C.U. 25) 150 to 200 m thick. During deposition of the cumulates, melting of wall and roof rock formed a layer of low-density, SiO_2-rich liquid at the roof of the chamber that is preserved as a xenolith-rich granophyric unit 0 to 70 m thick directly overlying C.U. 25 (*13, 14*); thus mafic and silicic liquids coexisted in a gravitationally stable configuration during crystallization of the mafic magma.

We measured isotopic ratios of Nd (^{143}Nd/^{144}Nd) and Sr (^{87}Sr/^{86}Sr) and concentrations of Rb, Sr, Sm, and Nd in samples spanning the uppermost cyclic unit (C.U. 25), the granophyric roof zone (GRZ), and the surrounding wall rocks (Table 1) (*15*). Initial Nd and Sr isotopic ratios (*16*) of cumulates are assumed to record the isotopic ratio of the magma from which they crystallized. Minor postcrystallization alteration had little effect on the Sm-Nd systematics but some effect on the Rb-Sr system, as demonstrated by the agreement of mineral and whole-rock initial ϵ_{Nd} values for sample 83DM-3 from C.U. 22 (Table 1) and the discordance of its respective ^{87}Sr/^{86}Sr values. However, because the relatively large whole-rock samples used in this study should average out millimeter-scale isotopic disturbances, we believe that the age-corrected ^{87}Sr/^{86}Sr ratios reflect magmatic values, as has been shown for other layered mafic complexes (*3, 4, 17*).

The ϵ_{Nd} and ^{87}Sr/^{86}Sr values of the GRZ fall intermediate between wall rock end-members and probably represent an average of the melted wall rock components (Fig. 1). Values of ^{87}Sr/^{86}Sr and ϵ_{Nd} for C.U. 25 samples lie within a much more restricted range (Fig. 1 inset and Fig. 2). The cumulates all have ϵ_{Nd} values of -0.75 (dashed line, Fig. 2), within analytical uncertainties, except the uppermost sample (83DM-11). In contrast, ^{87}Sr/^{86}Sr values increase with stratigraphic height (toward GRZ values) well outside of analytical error, from 0.7051 to 0.7097; only one sample (83DM-12) deviates from this trend. These data show that the C.U. 25 magma was progressively enriched in radiogenic Sr while its ϵ_{Nd} remained essentially constant.

To test whether bulk assimilation–fractional crystallization (AFC) models could account for the discrepancy between the Nd and Sr isotopic data, we constructed two models (*3, 4, 18*), one with a value for a (ratio of mass rate of assimilation to mass rate of crystallization) equal to zero, the other for $a = 0.12$. In the calculations we used the Nd and Sr concentrations and isotopic compositions of the GRZ for the assimilant, and a bulk (crystals + intercumulus liquid) distribution coefficient of Sr (K_{Sr}) equal to 1. We let K_{Nd} increase from 0.2 at the base of C.U. 25 to 0.8 at the top to reflect increasing amounts of trapped intercumulus liquid (*19, 20*). The AFC models could not account for both the Nd and Sr isotopic variations (Fig. 3A). The ^{87}Sr/^{86}Sr data require $a \geq 0.10$, while the ^{143}Nd/^{144}Nd data require $a \leq 0.05$.

Because of the well-established difference in diffusivities between Nd and Sr in silicate melts (*5, 6*), we next investigated the possibility that the isotopic variations were caused by diffusive contamination rather than bulk mixing. Baker (*7*) found that the elemental and isotopic effects of diffusive exchange between coexisting anhydrous rhyolite and dacite layers are small for time scales less than 10^5 to 10^6 years. However, recent diffusion experiments (*21*) show that Sr tracer diffusivities in wet rhyolites are large enough to allow significant isotopic exchange in geologically reasonable time scales.

We use the example of Sr isotopes to describe our model of isotopic exchange between two silicate liquid layers (*22*). The total concentration of Sr in each layer is assumed to evolve independently of the isotopic exchange across the interface. The concentration of Sr in the silicic layer (C_a) is taken to be constant; the concentration in the mafic layer (C_m) is controlled by fractional crystallization of the mafic magma. The compositional interface between the two layers is assumed to be infinitely sharp with respect to all components except ^{87}Sr (*23*). Diffusion of ^{87}Sr from the silicic magma to the mafic magma takes place through a boundary layer of thickness

Berkeley Center for Isotope Geochemistry, Department of Geology and Geophysics, University of California, and Earth Science Division, Lawrence Berkeley Laboratory, Berkeley, CA 94720.

---

*To whom correspondence should be addressed. Present address: Division of Geological and Planetary Sciences 170-25, California Institute of Technology, Pasadena, CA 91125.

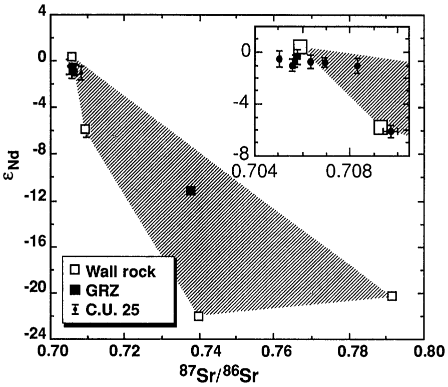

Fig. 1. Variations in initial (1257 Ma) $^{87}Sr/^{86}Sr$ and ϵ_{Nd} values for the Muskox intrusion and surrounding wall rocks. Sample M-156 from the granophyric roof zone (closed square) lies within the field (shaded region) defined by the various wall rocks around the intrusion (open squares). Cumulates from C.U. 25 (closed circles) show a significant spread in $^{87}Sr/^{86}Sr$ ratios but not in ϵ_{Nd} values (inset).

x, which lies entirely within the silicic magma layer (*24*). The flux of ^{87}Sr into the mafic liquid can then be written:

$$J_{87} = \frac{D_{Sr}\rho_a}{x}([^{87}Sr]_a - [^{87}Sr]^*_a) \qquad (1)$$

where $[^{87}Sr]^*_a$ is the concentration in moles per unit mass of ^{87}Sr in the silicic magma that would give it an $^{87}Sr/^{86}Sr$ ratio equal to that of the mafic layer, D_{Sr} is the diffusivity of Sr, and ρ_a is the density of the silicic magma. This equation can then be rewritten:

$$J_{87} = \frac{D_{Sr}\rho_a}{x}[^{86}Sr]_a(\epsilon_a - \epsilon_m) \qquad (2)$$

where we have used ϵ as shorthand for $^{87}Sr/^{86}Sr$. From this formulation, expressions for the rate of change of $^{87}Sr/^{86}Sr$ in the mafic and silicic liquids can be derived:

$$\frac{d\epsilon_m}{dt} = \frac{D_{Sr}\rho_a A C_a}{xFM_0C_m}(\epsilon_a - \epsilon_m) \qquad (3)$$

$$\frac{d\epsilon_a}{dt} = \frac{D_{Sr}\rho_a A}{xM_a}(\epsilon_m - \epsilon_a) \qquad (4)$$

where A is the interface area, and F is the fraction of mafic liquid remaining relative to the initial liquid mass M_0 (*25*). For the case of fractional crystallization with variable K, the rate of change of an element concentration in the mafic magma is given by

$$\frac{dC_m}{dt} = (K_{Sr} - 1)C_mF^{-1}\frac{dF}{dt} \qquad (5)$$

In order to solve Eqs. 3 and 5, the time dependence of crystallization within the mafic magma must be specified. In the modeling that follows, we assume that the rate of crystallization is proportional to the square root of time (*26, 27*); that is, $F = 1 - (t/t_c)^{1/2}$, where t is the time elapsed since initial injection of magma into the chamber and t_c is the total time of crystallization. The results are not strongly dependent on the crystallization law used. Equations 1 through 5 apply equally to Nd isotopes.

To model the effects of diffusional exchange combined with fractional crystallization (DFC) in the Muskox intrusion, we estimated values for the physical parameters and then used the variations of the model curves with t_c to constrain the crystallization time of the intrusion. We estimate that the thickness of the silicic portion of the chemical boundary layer is 0.1 m (*28*) and that the silicic magma contained 5% H_2O by weight. The silicic boundary layer was most likely heated to supersolidus temperatures by the underlying convecting mafic magma. Interpolating between Baker's (*21*) estimates of D_{Sr} in hydrous rhyolite at 1000°C of 1.5×10^{-12} m^2 s^{-1} at 3.5% H_2O and 2.3×10^{-11} m^2 s^{-1} at 6% H_2O and assuming that log D is proportional to the H_2O content for >2% H_2O (*21, 29*), we calculated a value of 8×10^{-12} m^2 s^{-1} for D_{Sr}. Lesher (*30*) showed that D_{Nd} in rhyolite is ~1/8 that of D_{Sr}, so we used $D_{Nd} = 1 \times 10^{-12}$ m^2 s^{-1}. The same values of K_{Sr} and K_{Nd} were used as in the AFC modeling. Nd and Sr isotopic ratios of the silicic liquid at $t = 0$ were chosen so that they would evolve to the values of GRZ by the end of the crystallization of the mafic liquid ($t = t_c$). The magnitudes of the isotopic shifts in the silicic magma are dependent on the mass of the silicic liquid layer. In the case of the Muskox intrusion, the ratio of silicic liquid mass to mafic liquid mass (M_a/M_m) must be greater than ~0.35 to obtain geologically reasonable silicic liquid isotopic compositions at $t = 0$ (*31*). We set $M_a/M_m = 0.35$ in the modeling described below.

For the chosen parameters, a crystallization time of 8000 years for the uppermost

Table 1. Sample locations, trace element concentrations, and isotopic data.

Sample	Location	Height* (m)	Sr (ppm)	Nd (ppm)	$^{87}Rb/^{86}Sr$†	Initial‡ $^{87}Sr/^{86}Sr$	±§	$^{147}Sm/^{144}Nd$‖	Initial‡ ϵ_{Nd}	±§
M-156	GRZ		98.7	50.87	5.55	0.73764	53	0.1133	−11.2	0.5
83DM-11	C.U. 25	163	155.3	33.58	3.08	0.70974	30	0.1291	−6.2	0.4
83DM-12	C.U. 25	155	186.9	54.16	1.227	0.70583	13	0.1363	−0.4	0.6
83DM-23	C.U. 25	133	293.9	25.67	0.598	0.70833	7	0.1432	−1.0	0.6
83DM-8	C.U. 25	111	332.8	26.92	0.382	0.70639	5	0.1462	−0.7	0.6
83DM-7	C.U. 25	89	310.1	23.03	0.336	0.70698	7	0.1458	−0.8	0.4
83DM-16	C.U. 25	57	312.7	22.29	0.286	0.70562	6	0.1377	−1.0	0.5
83DM-5	C.U. 25	42	229.6	8.05	0.1329	0.70567	3	0.1635	−0.7	0.5
83DM-4	C.U. 25	29	110.8	5.059	0.1311	0.70507	3	0.1745	−0.5	0.6
83DM-3	C.U. 22		342.3	10.04	0.0899	0.70535	3	0.1424	−0.3	0.4
Clinopyroxene			25.79	14.76	0.0963	0.70533	4	0.1861	−0.8	0.5
Orthopyroxene 1			2.24	0.905	0.313	0.70502	15	0.2587	−0.9	0.7
Orthopyroxene 2			2.6	1.118				0.2409	−0.5	0.5
Plagioclase			566.8	2.430	0.0608	0.70543	3	0.0882	−1.0	0.6
83DM-42a	Granite wall rock		58.54	41.07	15.23	0.79160	139	0.1078	−20.3	0.8
83DM-42b	Granite wall rock		84.4	119.9	7.49	0.73982	70	0.0855	−22.0	0.5
83DM-14	Hornfels wall rock		225.7	12.56	0.316	0.70594	5	0.1657	0.4	0.4
83DM-35	Orthogneiss wall rock		193.7	20.21	0.605	0.70933	7	0.1308	−5.8	0.5

*Stratigraphic height above base of C.U. 25. †Uncertainty ≤0.5% ‡Corrected to crystallization age of 1257 Ma (*16*). §Uncertainty includes ±2 SEM in ratio and uncertainty in $^{87}Rb/^{86}Sr$ or $^{147}Sm/^{144}Nd$. ‖Uncertainty ≤0.3%.

Fig. 2. Plots of $^{87}Sr/^{86}Sr$ ratios and ϵ_{Nd} values for C.U. 25 cumulates against stratigraphic height above the base of C.U. 25 and *F* (mass fraction of liquid remaining relative to initial liquid mass); *F* is assumed to be proportional to stratigraphic height in C.U. 25. All ϵ_{Nd} values fall within error of −0.75 (dashed line) except the uppermost sample (83DM-11); in contrast, $^{87}Sr/^{86}Sr$ values increase upward in the section.

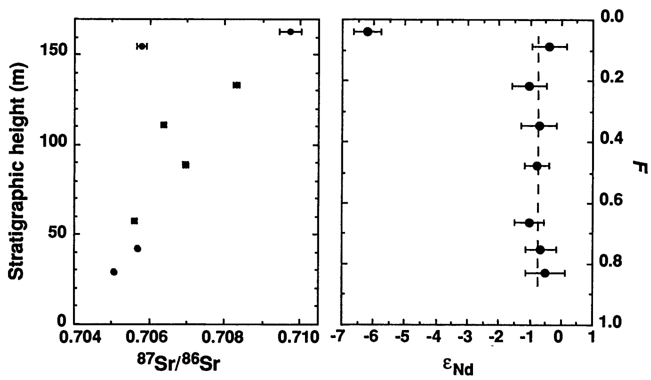

cyclic unit provides a reasonable fit to both the Sr and the Nd isotopic data (Fig. 3B). For comparison, neither 800-year nor 30,000-year crystallization times fit the Sr isotopic data, although any time less than 30,000 years makes an acceptable fit to the Nd data. A crystallization time of 30,000 years requires an initial silicic liquid $^{87}Sr/^{86}Sr$ value of 0.780, which is difficult to reconcile with the wall rock data. For t_c = 8000 years, the $^{87}Sr/^{86}Sr$ ratio of the silicic liquid shifts downward by 0.01 from an initial value of 0.748 at $t = 0$, well within the field of wall rock values (Fig. 1); the shift of ϵ_{Nd} in the silicic liquid is negligible. Because the underlying 24 cyclic units were formed by partial crystallization of earlier magma injections, the total lifetime of the Muskox magmatic system (including the surface flows from venting of the chamber) would then be on the order of 50,000 to 100,000 years. Additional modeling indicates that the results are not sensitive to the chosen partition coefficients, nor are they sensitive to the initial concentrations of Sr and Nd in the magma and assimilant, so long as realistic estimates are used. However, the magnitudes of the isotopic shifts caused by DFC are strongly dependent on the chosen values for diffusivity and boundary layer thickness (Eqs. 3 and 4). Improved understanding of boundary layer conditions should lead to more accurate estimates of crystallization times in cases where DFC has operated.

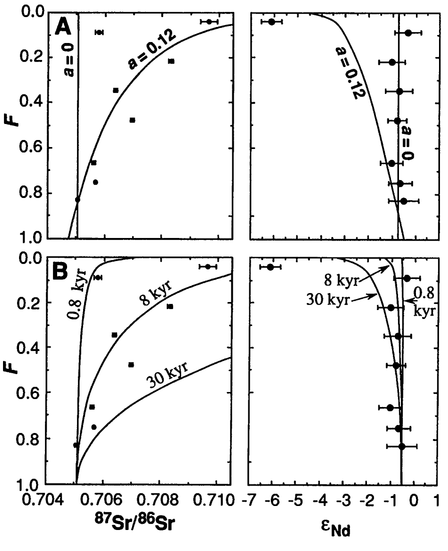

Fig. 3. (**A**) Isotopic evolution curves for AFC models compared to C.U. 25 data. Curves are shown for the cases of *a* equal to 0 and *a* = 0.12. *F* is the fraction of mafic liquid remaining in C.U. 25. (**B**) Isotopic evolution curves for DFC models compared to C.U. 25 data. The curves represent the isotopic evolution of the mafic magma as it diffusively exchanges with the overlying silicic magma. The numbers indicate the total crystallization time of C.U. 25 for each model; see text for other parameters.

At deeper crustal levels where crystallization times are likely to be much greater, the effects of diffusional isotopic exchange may be even larger than those observed in the Muskox intrusion. In Fig. 4, we constructed a model using hypothetical end-members to demonstrate the possible isotopic effects of DFC compared to those of AFC. The path for the AFC process with *a* = 0.1 is compared to the effects of DFC with t_c = 20,000 years for a sill of basaltic magma 200 m thick with isotopic ratios characteristic of mantle plumes (ϵ_{Nd} = 0, $^{87}Sr/^{86}Sr$ = 0.7045) interacting with typical Proterozoic granitic crust (ϵ_{Nd} = −20, $^{87}Sr/^{86}Sr$ = 0.720). Given a sufficiently lengthy crystallization time, it is clear that DFC can produce Sr isotopic effects comparable to AFC, while maintaining almost constant Nd isotopic ratios. Interpretation of a DFC trend as an AFC trend would lead to gross overestimates of the $^{87}Sr/^{86}Sr$ ratio or ϵ_{Nd} of the assimilant end-member. In some instances, AFC and DFC may operate simultaneously; in these cases, the path would be intermediate to the curves shown in Fig. 4. The magnitude of the DFC effects are directly proportional to t_c and inversely proportional to the thickness of the mafic magma chamber. The $^{87}Sr/^{86}Sr$ ratio of the silicic magma can be significantly modified as well, again with little change in its major- or trace-element chemistry. This effect is enhanced if the underlying mafic magma is repeatedly replenished by injections of fresh magma.

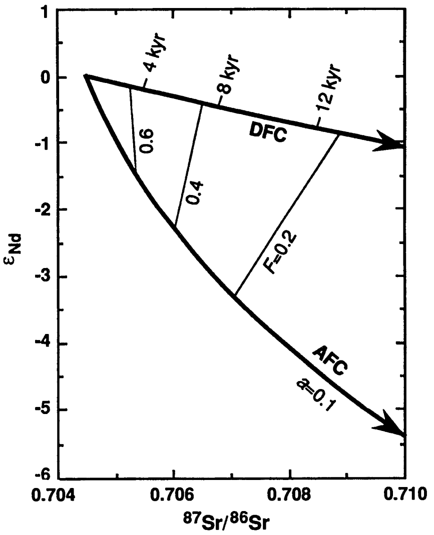

Fig. 4. Model curves for mafic magma (ϵ_{Nd} = 0, $^{87}Sr/^{86}Sr$ = 0.7045) interacting with Proterozoic granitic crust (ϵ_{Nd} = −20, $^{87}Sr/^{86}Sr$ = 0.720) for the processes of DFC and AFC. In the DFC model shown, the total crystallization time of the mafic magma is 20,000 years; the ticks along this curve indicate time passed since the initial intrusion of the magma. Tie lines represent equivalent values of *F* (mass fraction of mafic magma remaining in magma chamber).

The extent to which we can assume DFC operates in natural systems depends primarily on our estimates of the crystallization times of mafic magma chambers, which is contentious (*32*). However, the physical situation of silicic magma stably overlying mafic magma is likely to develop any time a basaltic magma ponds beneath less dense, low-melting granitic material, and in such cases physical mixing is thought to be inefficient. Thus, DFC should be considered in any interpretation of isotopic variations in basalts erupted through continental crust. In particular, shifts in $^{87}Sr/^{86}Sr$ ratios without corresponding shifts in $^{143}Nd/^{144}Nd$, commonly attributed to interaction with altered mafic crust, need to be reexamined. Although few experiments have been carried out on Pb diffusion in magmas, the relatively high diffusivity of Pb in minerals (*33, 34*) leads us to speculate that the effects of DFC on Pb isotopes in mafic magmas may be even larger than those exhibited by Sr. This is an additional factor to be considered in cases where Pb isotopic variations in igneous mafic rocks are large compared to those of Sr and Nd.

REFERENCES AND NOTES

1. I. H. Campbell and J. S. Turner, *J. Geol.* **95**, 155 (1987).

2. C. M. Oldenburg, F. J. Spera, D. A. Yuen, *Earth-Sci. Rev.* **29**, 331 (1990).
3. D. J. DePaolo, *J. Petrol.* **26**, 925 (1985).
4. B. W. Stewart and D. J. DePaolo, *Contrib. Mineral. Petrol.* **104**, 125 (1990).
5. M. Magaritz and A. W. Hofmann, *Geochim. Cosmochim. Acta* **42**, 595 (1978).
6. ______, *ibid.*, p. 847.
7. D. R. Baker, *Contrib. Mineral. Petrol.* **104**, 407 (1990).
8. ______, *Geochim. Cosmochim. Acta* **53**, 3015 (1989).
9. C. E. Lesher, *Nature* **344**, 235 (1990).
10. E. B. Watson and S. R. Jurewicz, *J. Geol.* **92**, 121 (1984).
11. A. F. Trial and F. J. Spera, *Int. J. Heat Mass Transfer* **31**, 941 (1988).
12. T. N. Irvine and C. H. Smith, in *Ultramafic and Related Rocks*, P. J. Wyllie, Ed. (Wiley, New York, 1967), pp. 38–49.
13. T. N. Irvine, *Geol. Soc. S. Afr. Spec. Publ.* **1**, 441 (1970).
14. Thickness of GRZ estimated from map and cross sections of C. H. Smith, T. N. Irvine, D. C. Findlay, *Geol. Surv. Can. Maps 1213-A* and *1214-A* (1966).
15. Sample M-156, collected from a xenolith-rich region just below the roof, was provided by T. N. Irvine; all other samples were collected by D.J.D. in a 1983 expedition. Stratigraphic positions of samples within C.U. 25 (Table 1) are estimated from their field relations and map locations and are given relative to the base of C.U. 25, which is assumed to have an average thickness of 170 m. Whole-rock samples of 100 to 500 g were crushed and split, and 100- to 500-mg aliquots were dissolved with HF + $HClO_4$. After spiking with tracer solutions of Rb, Sr, Sm, and Nd, the cations of interest were separated by standard ion-exchange techniques. Concentrations and isotopic ratios were determined by thermal ionization mass spectrometry, and all elements were run as metal species except Nd, which was run as NdO^+. Most measurements were carried out on VG single collector machines at the University of California, Los Angeles (UCLA) and the Berkeley Center for Isotope Geochemistry (BCIG), with some Sr isotopic analyses run on the BCIG VG multicollector. Both single-collector machines give the same values for $^{143}Nd/^{144}Nd$ within measurement uncertainties, and all $^{87}Sr/^{86}Sr$ ratios are corrected to the pre-1989 UCLA value for NBS987 of 0.71031.
16. All values of $^{87}Sr/^{86}Sr$ and ϵ_{Nd} quoted in the text are initial ratios (corrected for decay of ^{87}Rb and ^{147}Sm since the time of crystallization). In this study we assume a crystallization age of 1257 Ma (million years ago), based on an internal Sm-Nd isochron from a two-pyroxene gabbro collected from C.U. 22 (sample 83DM-3, Table 1); this age of 1257 ± 40 Ma (2σ) is within error of the U-Pb age of 1270 ± 4 Ma of A. N. LeCheminant and L. M. Heaman [*Earth Planet. Sci. Lett.* **96**, 38 (1989)]. Age-corrected Nd isotopic ratios are reported as ϵ_{Nd}, with
$$\epsilon_{Nd}(T) = 10^4\left(\frac{^{143}Nd/^{144}Nd_{SAMP}(T)}{^{143}Nd/^{144}Nd_{CHUR}(T)} - 1\right)$$
where T is the crystallization age of the Muskox intrusion and CHUR is the chondritic reservoir. The chondritic isotopic composition at time T is given by: $^{143}Nd/^{144}Nd_{CHUR}(T) = 0.511836 - 0.1967[\exp(\lambda_{Sm}T) - 1]$. Decay constants used are 0.0142 per 10^9 years for λ_{Rb} and 0.00654 per 10^9 years for λ_{Sm}.
17. R. E. Harmer and M. R. Sharpe, *Econ. Geol.* **80**, 813 (1985).
18. D. J. DePaolo, *Earth Planet. Sci. Lett.* **53**, 189 (1981).
19. T. N. Irvine, in *Physics of Magmatic Processes*, R. B. Hargraves, Ed. (Princeton Univ. Press, Princeton, NJ, 1980), pp. 325–383.
20. D. N. Shirley, *J. Geol.* **94**, 795 (1986).
21. D. R. Baker, *Contrib. Mineral. Petrol.* **106**, 462 (1991).
22. In our model, we assume that the coexisting magmas achieve a steady-state condition of two-layer convection on a time scale that is short relative to the time scale of crystallization. This is a particularly good assumption for the Muskox intrusion, because the GRZ was already in a convective state when the final pulse of mafic magma was emplaced. For further discussion of the relevant magma chamber dynamics, see C. M. Oldenburg, F. J. Spera, D. A. Yuen, and G. Sewell [*J. Geophys. Res.* **94**, 9215 (1989)] and B. D. Marsh [*J. Petrol.* **30**, 479 (1989)]; see also discussion of Marsh's paper by H. E. Huppert and J. S. Turner [*ibid.* **32**, 851 (1991)].
23. To maintain constant Sr concentration in the silicic liquid, there must be a net flow of the other Sr isotopes (^{88}Sr, ^{86}Sr, and ^{84}Sr) into the silicic liquid to balance the loss of ^{87}Sr. This can be ignored for our purposes because the total change in $[^{86}Sr]_a$ is only about 0.1% (see Eq. 2).
24. The boundary layer would in fact consist of both mafic and silicic components; however, diffusivities of Sr and Nd in basalt are faster by up to an order of magnitude than diffusivities in rhyolite (*5, 6*), making diffusion in the silicic portion of the boundary layer the rate-limiting process.
25. In Eqs. 3 and 4, we use the approximation that the concentration of Sr is independent of the $^{87}Sr/^{86}Sr$ ratio ($[^{86}Sr]/[Sr]$ = constant), which is generally accurate to better than 0.5%.
26. J. C. Jaeger, *Am. J. Sci.* **255**, 306 (1957).
27. T. N. Irvine, *Can. J. Earth Sci.* **7**, 1031 (1970).
28. S. Clark, F. J. Spera, D. A. Yuen, in *Magmatic Processes: Physicochemical Principles*, B. O. Mysen, Ed. (Geochemical Society, University Park, PA, 1987), pp. 289–305.
29. T. M. Harrison and E. B. Watson, *Contrib. Mineral. Petrol.* **84**, 66 (1983).
30. C. E. Lesher, *Trans. Am. Geophys. Union* **72**, 309 (1991).
31. In order to supply enough Sr to produce the increase in $^{87}Sr/^{86}Sr$ observed in C.U. 25, the roof zone of molten wall rock overlying the Muskox cumulates must have been more extensive during crystallization than the current exposure would suggest. Two possible explanations are that (i) the GRZ thickens to the north of the current Muskox exposure where the intrusion dips beneath sedimentary cover, or (ii) much of the GRZ was vented during and after crystallization of the mafic magma. The lack of a downward-crystallizing roof sequence in the Muskox intrusion, even in regions where wall rock breccia is not present, suggests that such a liquid layer was present throughout the entire roof zone during crystallization of the cumulates.
32. For contrasting views, see H. E. Huppert and R. S. J. Sparks [*J. Petrol.* **29**, 599 (1988)] and A. N. Halliday *et al.* [*Earth Planet. Sci. Lett.* **94**, 274 (1989)], as well as discussion by R. S. J. Sparks, H. E. Huppert, and C. J. N. Wilson [*ibid.* **99**, 387 (1990)].
33. J. M. Mattinson, *Contrib. Mineral. Petrol.* **67**, 233 (1978).
34. E. B. Watson, T. M. Harrison, F. J. Ryerson, *Geochim. Cosmochim. Acta* **49**, 1813 (1985).
35. We thank T. N. Irvine for samples and field assistance. The comments of R. C. Capo, R. B. Hanson, F. M. Richter, F. J. Spera, and an anonymous reviewer improved the manuscript. This work was supported by NSF grants EAR84-15143 and EAR88-04609.

11 October 1991; accepted 2 December 1991

Reaction Planning: Computer-Aided Discovery of a Novel Elimination Reaction

RAINER HERGES* AND CHRISTOPH HOOCK

Algorithms based on graph theory and implemented in a computer program have been used to search for unprecedented reactions. This approach is illustrated by a systematic and exhaustive screening of pericyclic reactions in order to find new reactions useful in the synthesis of conjugated dienes. Two reactions were found. They were optimized by structural variation with the aid of quantum-chemical calculations and were then experimentally verified.

MOST DISCOVERIES OF THE IMPORTANT synthetic organic reactions have been serendipitous (*1*). For example, the Wittig reaction, H. C. Brown's hydroboration, and low-pressure polymerization of ethylene were not designed with the aim of synthesizing or functionalizing olefins or polymerizing ethylene but were discovered during experiments based on completely different ideas (*2*). In contrast to the case of synthesis planning (*3*), there are few general problem-solving strategies available to "invent" chemical reactions. Recently, a general methodology for the systematic search and design of organic reactions was reported. The task of finding the complete set of basic reaction schemes that comply with a given mechanism can be reduced to a graph-theoretical problem (*4*). A similar algorithm has been implemented in the program IGOR (*5*). The methods are used to thoroughly screen areas of organic chemistry for unprecedented reactions (*6–8*). The search, design, and experimental verification of two reactions aimed at the synthesis of conjugated dienes serve as an example.

Conjugated dienes are important in general organic synthesis and polymer chemistry. Because pericyclic reactions are usually stereoselective, this class of reactions was selected as the search area for new synthetic methods. Generation of the complete set of conceivable pericyclic reactions with three to six atoms, four to six electrons, and a maximum of one lone pair involved in the transition state yielded 44 basic reaction schemes (*8*), of which 5 are suitable for the synthesis of dienes: electrocyclic ring-

---

Institut für Organische Chemie, Universität Erlangen-Nürnberg, Henkestraße 42, 8520 Erlangen, Germany.

*To whom correspondence should be addressed.